CrossMark
← click for updates

The Birmingham parallel genetic algorithm and its application to the direct DFT global optimisation of Ir$_N$ (*N* = 10–20) clusters†

Jack B. A. Davis,*[a] Armin Shayeghi,[b] Sarah L. Horswell[a] and Roy L. Johnston*[a]

A new open-source parallel genetic algorithm, the Birmingham parallel genetic algorithm, is introduced for the direct density functional theory global optimisation of metallic nanoparticles. The program utilises a pool genetic algorithm methodology for the efficient use of massively parallel computational resources. The scaling capability of the Birmingham parallel genetic algorithm is demonstrated through its application to the global optimisation of iridium clusters with 10 to 20 atoms, a catalytically important system with interesting size-specific effects. This is the first study of its type on Iridium clusters of this size and the parallel algorithm is shown to be capable of scaling beyond previous size restrictions and accurately characterising the structures of these larger system sizes. By globally optimising the system directly at the density functional level of theory, the code captures the cubic structures commonly found in sub-nanometre sized Ir clusters.

1. Introduction

Nanosized materials are currently being investigated for potential use in a variety of applications. This is because the nanosizing effects seen in such materials result in properties different from those of the bulk material. These properties can also be tuned, normally through altering the size and shape of the cluster.

Metallic nanoparticles are such materials, with potential optical, magnetic and catalytic applications.[1] Small Ir nanoparticles, in particular, are currently used as catalysts for a range of organic reactions, including olefin hydrogenation, oligomerisation, and ring-opening of cycloalkanes.[2] Ir has been shown both experimentally[3] and theoretically[4] to exhibit significant nanosize-induced hydrogen adsorption capacity. Larger Ir nanoparticles have been shown to be active in C–C bond hydrogenolysis.[5] Selective molecular recognition has also been seen in supported Ir cluster-based catalysts.[6]

A key step in rationalising properties, such as the catalytic activity of nanoparticles, is their structural characterisation. To achieve this it is necessary to sample comprehensively the potential energy landscape (PES) of the nanoparticle. A wide

variety of methods is available for the exploration of the PES. These methods include statistical mechanical methods, such as the CBEV/FCEM method,[7,8] basin-hopping methods,[9] such as GMIN,[10] and genetic algorithms, such as the Birmingham cluster genetic algorithm (BCGA).[11] The choice of method largely depends on the size and complexity of the system.

It is necessary to decide the level of theory required to replicate accurately a particular PES of a system. For example, the electronic structure of larger nanoparticles is thought to resemble closely that of the bulk material. This means the use of empirical potentials, such as the Gupta potential,[12] is suitable for the accurate representation of the PES. Statistical mechanical methods, such as CBEV/FCEM, may be best suited to these larger systems.[8] However, for smaller, sub-nanometre clusters a much more computationally demanding quantum mechanical description of the cluster PES is necessary as quantum-size effects, such as spin–orbit coupling, tend to dominate.[13–15] A variety of methods has been developed to achieve this, many of which have been outlined by Heiles and Johnston.[16]

The cubic structures adopted by sub-nanometre Ir clusters have been previously shown up to the CCSD(T) level of theory,[17–24] differing from the *fcc* structure of the bulk material. It is therefore vital that any global optimisation of Ir$_N$ (*N* = 10–20) structures is performed directly at the density functional theory (DFT) level of theory at least.

A quantum description of the PES greatly increases the cost of exploring it comprehensively, limiting the size of the cluster it is possible to investigate.[16] It is therefore necessary that

[a]*School of Chemistry, University of Birmingham, Birmingham, B15 2TT, UK. E-mail: jbad90@gmail.com, r.l.johnston@bham.ac.uk; Tel: +44 (0)1214 147477*
[b]*Eduard-Zintl-Institut, Technische Universität Darmstadt, Alarich-Weiss-Straße 8, 64287 Darmstadt, Germany. E-mail: shayeghi@cluster.pc.chemie.tu-darmstadt.de*
†*Electronic supplementary information (ESI) available. See DOI: 10.1039/ C5NR03774C*

efficient parallel methodologies, with the ability to utilise greater computational resources, are developed. There have been several implementations of parallel schemes within genetic algorithms for both atomic and molecular clusters but few combine this parallelism with direct DFT global optimisation.[25–29]

This work presents the global optimisation of Ir_N (N = 10–20) clusters directly at the DFT level of theory. This is achieved using the Birmingham parallel genetic algorithm (BPGA), a new open-source genetic algorithm available *via* Bitbucket.[30] The BPGA utilises a pool genetic algorithm methodology combined with the evaluation of potential cluster geometries in parallel.[25] This combination ensures highly efficient scaling when compared with generation based genetic algorithms and allows the structural characterisation of larger and more complex systems. The pool methodology has been recently applied to metallic clusters[31] and was benchmarked and applied successfully to the global optimisation of the much studied Au_{10} and Au_{20} clusters.[31] Its predictions for $Ag_{10}{}^+$ have also been shown to be accurate when compared with spectra from molecular beam experiments.[32] The BPGA incorporates this highly efficient algorithm within a flexible Python framework.

Due to the $5d^7 6s^2$ ground state and other low lying states originating from its $5d^8 6s^1$ configuration,[33] the spin of the Ir_N clusters must be considered in the calculations.[33] To account for this, spin-polarised DFT global optimisations are performed. The use of spin-polarised local minimisations effectively doubles the computational cost and can only now be performed due to the parallelism of the BPGA.

The BPGA is also capable of globally optimising bimetallic nanoalloys, whose PES is complicated by the presence of homotops.[34] It is hoped that this work demonstrates that scaling capability of the BPGA and its ability to utilise massively parallel architectures, which enable the program to predict accurately the geometries of metallic nanoparticles.

2. Methodology

2.1. Birmingham parallel genetic algorithm

The BPGA is a parallel genetic algorithm for the structural characterisation of nanoparticles. The program is written in object-oriented Python. This allows greater flexibility and the ability to utilise the large existing libraries of Python code, such as the atomic simulation environment.[35] Python is well suited to job submission, required by the DFT interface, on a large shared HPC resource, such as ARCHER.[36] The program is open-source and available *via* BitBucket.[30]

The BPGA utilises a pool methodology, shown in Fig. 1.[25,31] This differs from a generation-based code, where structures belong to and are evaluated generation by generation. When executed in parallel, multiple instances of the BPGA are started sequentially within a run. Each instance is a separate BPGA run with its own set of processes. The BPGA initially generates a fixed-size pool of n random geometries and places
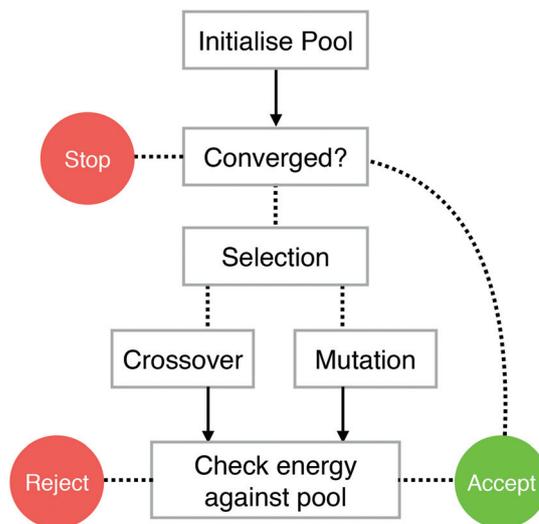

Fig. 1 The pool scheme used by the BPGA. Arrows represent DFT local minimisations.

them in a central database file which is available to the other instances of the program. In the present study the pool is set to n = 15 random geometries. These initial geometries are fixed so that no two atoms are overlapping.

In the local minimisation the energy of a structure is minimised with respect to its coordinates. This transforms the PES into a simpler stepped surface, greatly reducing the search space. If an instance becomes free and all structures in the pool are being or have been minimised the instance will continue to evaluate further random structures. If one of these new structures is lower in energy than the highest energy cluster in the pool, the new lower energy structure will replace it.

Once the initial pool of structures has been minimised, offspring and mutants are produced through crossover and mutation. The choice of producing either an offspring or mutant is based on the mutation rate, which is set to anywhere between 0–100% of the fixed pool size. In the present work the mutation rate is set to 10%.

Mutation is defined as the selection of a cluster at random from the pool and the displacement of two of its atoms by up to 1 Å. Other mutations schemes are available in the code, including generating a new random geometry or, for bimetallic systems, swapping unlike atoms.

Selection for crossover is carried out using the tournament method. Once selected, clusters undergo crossover according to the Deaven and Ho cut and splice method.[37] The cutting plane is weighted based on the fitness of each of the clusters selected. A higher fitness represents a lower energy.

A local minimisation of the offspring is performed and its energy is checked against those of the other structures in the pool. If the offspring's energy is lower than that of the highest energy structure in the pool, the offspring structure replaces it. Convergence is achieved when the energies of the structures in

the pool differ by no less than 10^{-3} eV. For larger clusters, convergence may not be achievable. In this case the lowest energy structure in the pool after a run of around 500 separate minimisations is taken as the putative global minimum.

The BPGA also has the ability to perform a DFT-level global optimisation of a cluster supported on a surface. This method, within a generation based code, has been demonstrated previously.[38]

2.2. DFT

Gamma-point, spin-polarised DFT calculations were performed with VASP.[39–43] Projected-augmented wave (PAW) pseudopotentials were used with the PBE exchange correlation functional.[44,45] A plane-wave basis set with a cut-off of 400 eV was used. Methfessel–Paxton smearing, with a sigma value of 0.01 eV, was utilised to improve metallic convergence.[46]

2.3. Energetics

The binding energies per atom were calculated using

$$E_b = \frac{1}{N}(E_{Ir_N} - NE_{Ir}), \tag{1}$$

where N is the total number of atoms, E_{Ir_N} is total energy of an N-atom Ir cluster and E_{Ir} is the energy of a spin-polarised Ir atom.

The stability of the clusters, relative to their $N + 1$ and $N - 1$ neighbours, is given by their second-order differences $\Delta^2 E$, calculated using

$$\Delta^2 E = 2E_{Ir_N} - (E_{Ir_{N+1}} + E_{Ir_{N-1}}). \tag{2}$$

3. Results

The BPGA calculations were performed on the UK's national supercomputer ARCHER.[36] Each was run in parallel with eight instances of the code operating on the pool. The theoretical scaling of this parallel pool methodology has been shown previously.[31] Around 500 structures were evaluated for each cluster size. Due to the high computational cost of the calculations multiple runs are not possible for each system size.

The parallelism within the code, and the scaling capabilities of VASP on ARCHER, allows for spin-polarised calculations to be carried out during the global optimisation. The binding energies E_b, point groups and spin multiplicities of the putative global minimum are given in Table 1. The coordinates of the global minima and the additional minima discussed are supplied in the ESI.†

Overall, the putative global minima from the BPGA searches are in good agreement with structures suggested in previous work on Ir clusters.[18,21–23] Some structures have been previously characterised and give a good indication of the ability of the BPGA to find the putative global minimum at a given level of theory. Other structures are reported here for the first time.

Table 1 Binding energies E_b, point groups and multiplicities ($2S + 1$) for the putative global minimum of Ir_N ($N = 10$–20) clusters

Cluster	Point group	E_b/eV	$(2S + 1)$
Ir_{10}	C_s	−4.914	3
Ir_{11}	C_1	−4.932	4
Ir_{12}	D_{4h}	−5.172	3
Ir_{13}	C_s	−5.139	4
Ir_{14}	C_s	−5.220	3
Ir_{15}	C_{2v}	−5.206	2
Ir_{16}	C_s	−5.301	3
Ir_{17}	C_s	−5.348	4
Ir_{18}	D_{4h}	−5.452	7
Ir_{19}	C_1	−5.416	2
Ir_{20}	C_1	−5.436	3
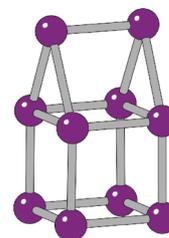
Ir_{10}

Fig. 2 The dimer-capped ("house") structure of Ir_{10}.

The BPGA successfully finds the C_{2v} dimer-capped ("house") structure, shown in Fig. 2, as the putative global minimum for Ir_{10} and scales successfully well beyond this previous 10-atom limit. The putative global minimum structures of Ir_N ($N = 11$–20) clusters are shown in Fig. 3.

The overall global minimum structure for Ir_{11} is a triangle-capped cube. This structure, together with a second highly competitive low lying minimum, an edge-bridged structure based on the Ir_{10} "house", are shown in Fig. 4. The two structures differ by 0.05 eV. The global minimum structure is a high spin structure with a spin multiplicity of 4, compared with the competitive minimum's multiplicity of 2. The spin polarised DFT global optimisation has allowed this lower energy putative global minimum to be reported for the first time.

The additional Ir in Ir_{12} now makes it possible to complete a third cubic face and the $3 \times 2 \times 2$ D_{2h} cuboid structure becomes the global minimum. For Ir_{13} the extra Ir bridges an edge on one of the cubes.

It was thought that the global minimum structure for Ir_{13} may be a C_{4v} structure, with an Ir atom capping an end of the cuboid, and that the cubic bounding cell used to generate the initial random geometries may have biased the search against any elongated structures. Local minimisations were carried out on C_{2v} centre edge-bridged, C_s top edge-bridged and C_{4v} top-capped cuboid structures, shown in Fig. 5. The C_{2v} centre edge-bridged structure locally minimises into a face-capped C_s structure. The structures were found to lie 0.26, 0.33 and 0.97
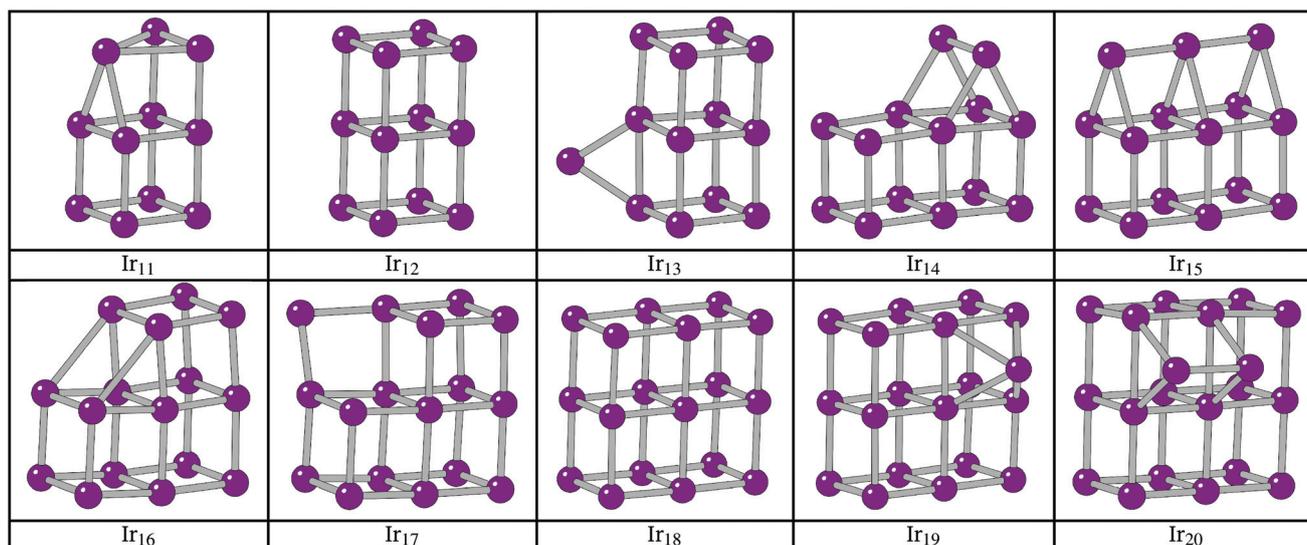
Fig. 3 Putative global minimum structures for Ir_N (N = 10−20) from the BPGA searches.

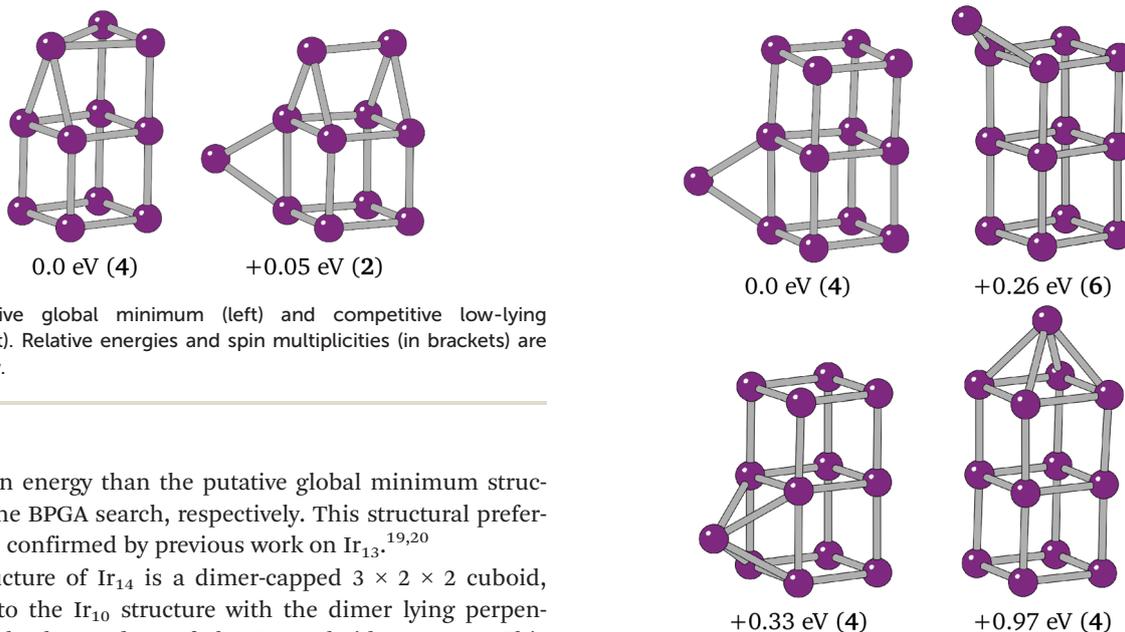0.0 eV (**4**)   +0.05 eV (**2**)

Fig. 4 Putative global minimum (left) and competitive low-lying minima (right). Relative energies and spin multiplicities (in brackets) are shown below.

0.0 eV (**4**)   +0.26 eV (**6**)

+0.33 eV (**4**)   +0.97 eV (**4**)

Fig. 5 Global minimum (top-left), top edge-bridged (top-right), centre edge-bridged (bottom-left) and top-capped (bottom-right) cubic structures assessed for Ir_{13}. The centre edge-bridged structure is shown after local minimisation to the face-capped cuboid structure.

eV higher in energy than the putative global minimum structure from the BPGA search, respectively. This structural preference is also confirmed by previous work on Ir_{13}.[19,20]

The structure of Ir_{14} is a dimer-capped $3 \times 2 \times 2$ cuboid, analogous to the Ir_{10} structure with the dimer lying perpendicular to the long edges of the Ir_{12} cuboid structure. This structure has been previously shown.[21] Upon addition of an extra Ir, the structure of Ir_{15} becomes a trimer-capped cuboid, with the Ir_3 trimer lying parallel to the long sides of the rectangular face.

The preference of Ir_{16} is shown to be a slightly deformed L-shaped cubic structure, so that two elongated 3.1 Å bonds can form between two cubes of the structure. Cubic bounding may also have affected Ir_{16}, as it follows from the structure of Ir_8, a cube, and Ir_{12} that the global minimum could be a $4 \times 1 \times 1$ cuboid. This structure was assessed alongside two other low-lying minima, T-capped and square-capped cuboid structures. The structures and relative energies of these minima are shown in Fig. 6, with the $4 \times 1 \times 1$ cuboid found to lie 0.88 eV higher in energy than the BPGA global minimum.

The structure of Ir_{17} shows the additional Ir in between two cubes of the Ir_{16} cuboid, the start of a complete $3 \times 3 \times 2$ cuboid. The additional Ir of Ir_{18} sits between two cubes of the L-shaped Ir_{17} cluster and forms the complete $3 \times 3 \times 2$ cuboid.

The extra Ir in Ir_{19} caps a cubic face on the $3 \times 3 \times 2$ cuboid. This putative global minimum was tested against an edge-bridged structure, which was believed to be the more likely global minimum structure following the trend seen in smaller
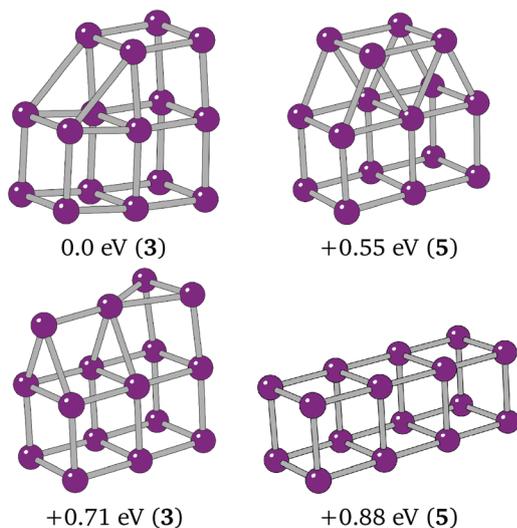
Fig. 6   Putative global minimum (top-left), $4 \times 1 \times 1$ cuboid, T-capped and square capped $3 \times 1 \times 1$ cubic structures assessed for Ir_{16}.

Fig. 8   Binding energies E_b, for Ir_N ($N = 10-20$) clusters.
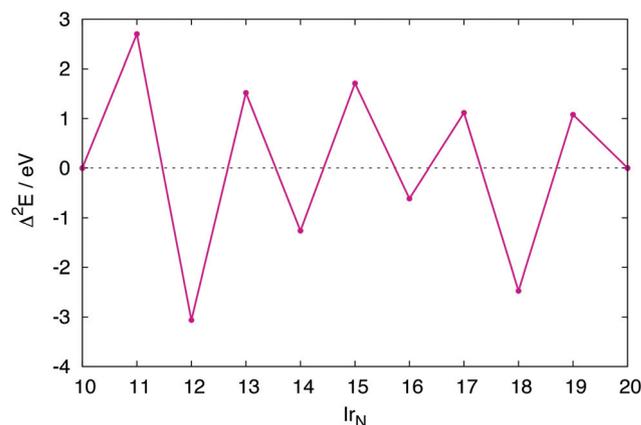
Fig. 9   Second-order differences $\Delta^2 E$, for Ir_N ($N = 10-20$) clusters.

clusters. The C_1 edge-bridged structure, shown in Fig. 7, was found to have a spin multiplicity of 6 and to be just 0.008 eV lower in energy than the BPGA global minimum.

The energetic differences between the low lying minima of Ir_{11} and Ir_{19} are far smaller than that seen for the various Ir_{13} minima and smaller than the error in the current DFT calculations. To determine accurately the global minimum, higher level calculations, coupled with experiment, will be required in the future.

The structure of Ir_{20} is analogous to that of Ir_{13} with an Ir_2 dimer lying perpendicular to the long edges of the $3 \times 3 \times 2$ cuboid structure.

The binding energies of the clusters give an indication of the relative stability of the clusters, with more negative values indicating greater stability. E_b values are shown in Fig. 8. Overall, E_b tends to decrease as N increases, with Ir_{18} having the lowest E_b.

For several N-atom clusters E_b is higher (less stable) than for the $N - 1$ cluster: in particular Ir_{13}, Ir_{15} and Ir_{19}. Ir_{20}, despite Ir forming a dimer capping a face, has a higher E_b
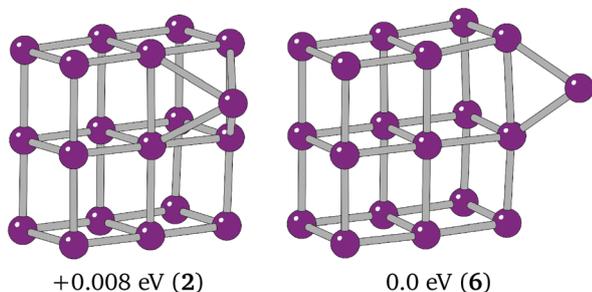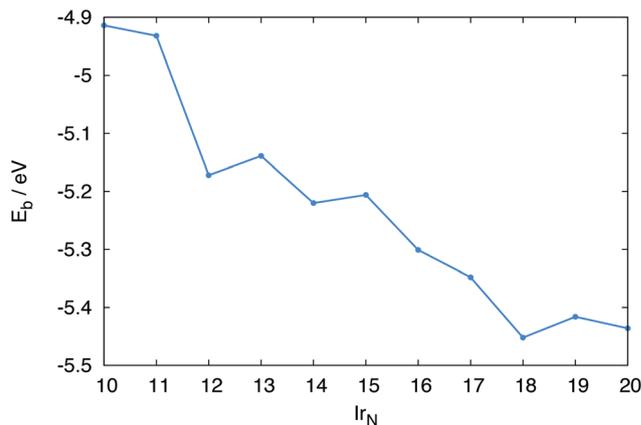
than Ir_{18}. The increased stability displayed by the even numbered clusters is more clearly shown by their second-order difference plot shown in Fig. 9. Each odd numbered cluster clearly shows decreased stability, indicated by a positive $\Delta^2 E$, relative to its even numbered neighbours.

The spin multiplicities of the clusters are given in Table 1. All global minima are found to have multiplicities of between 2 and 7. This is a clear indication of the importance of magnetic effects in these clusters. In particular, high spin structures are shown to be the global minimum structures of Ir_{11} and Ir_{19}. It is likely that these and other low energy minima would have been excluded from the searches if non-spin-polarized calculations had been carried out.

4.   Conclusions

The BPGA has successfully coupled the computation resources of ARCHER[36] with the scaling capability of a pool genetic algorithm methodology. This has allowed the direct DFT global optimisation of Ir_N ($N = 10-20$) clusters, with some

Fig. 7   Putative global minimum (left) and edge-bridged cuboid structure for Ir_{19}.

global minimum structures being reported here for the first time.

The code has captured the cubic nature of the sub-nanometre Ir clusters with the putative global minima evaluated and compared with previous results. For Ir_{11} and Ir_{19} their spin has been shown to determine their global minimum structures, which would have otherwise been missed in a low-spin search. The use of spin polarized calculations has been made possible because of the BPGA's ability to utilise greater computational resources. The structural characterisation of a system is a vital first step in exploring its catalytic properties. The structures of the Ir_N clusters will form the basis of future studies of the catalytic properties of the system, including modelling their interaction with small molecules.

The cubic structures found here are in agreement with higher level CCSD(T) and CASSCF calculations on Ir_8, reported by Dixon et al.[18] In future work, we will investigate the effect of changing the functional in DFT calculations on Ir clusters; in particular we will explore the use of meta-GGA functionals.[47,48]

The development of the BPGA will continue. This will include the implementation of new features, such as the global optimisation of a system in the presence of a ligand or directly on a variety of surfaces. Further improvements to the efficiency of the parallel scheme will also be made. The code will be applied to a variety of new supported and ligated mono- and bimetallic cluster systems. The number of interfaces to common quantum chemistry programs within the BPGA will be expanded and applied to the global optimisation of systems at theory levels beyond DFT.

Acknowledgements

References

1 R. Ferrando, J. Jellinek and R. L. Johnston, Chem. Rev., 2008, 108, 845–910.

2 A. Uzun, D. A. Dixon and B. C. Gates, ChemCatChem, 2011, 3, 95–107.

3 H. Kobayashi, M. Yamauchi and H. Kitagawa, J. Am. Chem. Soc., 2012, 134, 6893–6895.

4 J. B. A. Davis, S. L. Horswell, L. Piccolo and R. L. Johnston, J. Organomet. Chem., 2015, DOI: 10.1016/j.jorganchem.2015.04.03.

5 L. Piccolo, S. Nassreddine, G. Toussaint and C. Geantet, ChemSusChem, 2012, 5, 1717–1723.

6 A. Okrut, R. C. Runnebaum, X. Ouyang, J. Lu, C. Aydin, S.-J. Hwang, S. Zhang, O. A. Olatunji-Ojo, K. A. Durkin, D. A. Dixon, B. C. Gates and A. Katz, Nat. Nanotechnol., 2014, 9, 459–465.

7 M. Polak and L. Rubinovich, Surf. Sci., 2005, 584, 41–48.

8 J. B. A. Davis, R. L. Johnston, L. Rubinovich and M. Polak, J. Chem. Phys., 2014, 141, 224307.

9 D. Wales and J. P. K. Doye, J. Phys. Chem. A, 1997, 101, 5111–5116.

10 http://www-wales.ch.cam.ac.uk/GMIN/.

11 R. L. Johnston, Dalton Trans., 2003, 4193–4207.

12 F. Cleri and V. Rosato, Phys. Rev. B: Condens. Matter, 1993, 48, 22–33.

13 S. Heiles, A. J. Logsdail, R. Schäfer and R. L. Johnston, Nanoscale, 2012, 4, 1109–1115.

14 C. J. Heard and R. L. Johnston, Eur. Phys. J. D, 2013, 67, 34.

15 P. C. Jennings and R. L. Johnston, Comput. Theor. Chem., 2013, 1021, 91–100.

16 S. Heiles and R. L. Johnston, Int. J. Quantum Chem., 2013, 113, 2091–2109.

17 Y. Chen, M. Huo, T. Chen, Q. Li, Z. Sun and L. Song, Phys. Chem. Chem. Phys., 2015, 17, 1680–1687.

18 M. Chen and D. A. Dixon, J. Phys. Chem. A, 2013, 117, 3676–3688.

19 M. J. Piotrowski, P. Piquini, M. M. Odashima and J. L. Da Silva, J. Chem. Phys., 2011, 134, 134105.

20 M. Zhang and R. Fournier, Phys. Rev. A, 2009, 79, 043203.

21 J. Du, X. Sun, J. Chen and G. Jiang, J. Phys. Chem. A, 2010, 114, 12825–12833.

22 T. Pawluk, Y. Hirata and L. Wang, J. Phys. Chem. B, 2005, 109, 20817–20823.

23 W. Zhang, L. Xiao, Y. Hirata, T. Pawluk and L. Wang, Chem. Phys. Lett., 2004, 383, 67–71.

24 G. Ping, Z. Ji-Ming, Z. Pei, Z. Lin-Lin and R. Zhao-Yu, Chin. Phys. B, 2010, 19, 083601.

25 B. Bandow and B. Hartke, J. Phys. Chem. A, 2006, 110, 5809–5822.

26 L. B. Vilhelmsen and B. Hammer, J. Chem. Phys., 2014, 141, 044711.

27 Y. Ge and J. D. Head, J. Phys. Chem. B, 2004, 108, 6025–6034.

28 J. M. Dieterich and B. Hartke, Mol. Phys., 2010, 108, 279–291.

29 F. Weigend, J. Chem. Phys., 2014, 141, 134103.

30 https://bitbucket.org/JBADavis/bpga/.

31 A. Shayeghi, D. Götz, J. B. A. Davis, R. Schäfer and R. L. Johnston, Phys. Chem. Chem. Phys., 2015, 17, 2104–2112.

32 A. Shayeghi, R. L. Johnston and R. Schäfer, J. Chem. Phys., 2014, 141, 181104.

33 J. E. Sansonetti and W. C. Martin, J. Phys. Chem. Ref. Data, 2005, 34, 1777–1781.

34 J. Jellinek and E. B. Krissinel, Chem. Phys. Lett., 1996, 258, 283–292.

35 https://wiki.fysik.dtu.dk/ase/.

36 http://www.archer.ac.uk.

37 D. M. Deaven and K. M. Ho, *Phys. Rev. Lett.*, 1995, **75**, 288–291.

38 C. J. Heard, S. Heiles, S. Vajda and R. L. Johnston, *Nanoscale*, 2014, **6**, 11777–11788.

39 G. Kresse and J. Hafner, *Phys. Rev. B: Condens. Matter*, 1993, **47**, 558–561.

40 G. Kresse and J. Hafner, *Phys. Rev. B: Condens. Matter*, 1994, **49**, 14251–14269.

41 G. Kresse and J. Furthmüller, *Comput. Mater. Sci.*, 1996, **6**, 15–50.

42 G. Kresse and J. Furthmüller, *Phys. Rev. B: Condens. Matter*, 1996, **54**, 11169–11186.

43 H. J. Monkhorst and J. D. Pack, *Phys. Rev. B: Solid State*, 1976, **13**, 5188–5192.

44 J. Perdew, K. Burke and Y. Wang, *Phys. Rev. B: Condens. Matter*, 1996, **54**, 533–539.

45 G. Kresse and D. Joubert, *Phys. Rev. B: Condens. Matter*, 1999, **59**, 1758–1775.

46 M. Methfessel and A. T. Paxton, *Phys. Rev. B: Condens. Matter*, 1989, **40**, 3616–3621.

47 L. A. Constantin, E. Fabiano and F. Della Sala, *J. Chem. Theory Comput.*, 2013, **9**, 2256–2263.

48 P. Hao, J. Sun, B. Xiao, A. Ruzsinszky, G. I. Csonka, J. Tao, S. Glindmeyer and J. P. Perdew, *J. Chem. Theory Comput.*, 2013, **9**, 355–363.